

Global and regional assessment of sustained inflation pressure-volume curves in patients with acute respiratory distress syndrome

T Becher¹, P Rostalski², M Kott¹, A Adler³, D Schädler¹, N Weiler¹ and I Frerichs¹

¹ Department of Anaesthesiology and Intensive Care Medicine, University Medical Centre Schleswig-Holstein, Campus Kiel, Kiel, Germany

² Institute for Electrical Engineering in Medicine, Lübeck University, Lübeck, Germany

³ Systems and Computer Engineering, Carleton University, Ottawa, Ontario, Canada

E-mail: tobias.becher@uksh.de

Abstract. Static or quasi-static pressure-volume (P-V) curves can be used to determine the lung mechanical properties of patients suffering from acute respiratory distress syndrome (ARDS). According to the traditional interpretation, lung recruitment occurs mainly below the lower point of maximum curvature (LPMC) of the inflation P-V curve. Although some studies have questioned this assumption, setting of positive end-expiratory pressure 2 cmH₂O above the LPMC was part of a “lung-protective” ventilation strategy successfully applied in several clinical trials. The aim of our study was to quantify the amount of unrecruited lung at different clinically relevant points of the P-V curve. P-V curves and electrical impedance tomography (EIT) data from 30 ARDS patients were analysed. We determined the regional opening pressures for every EIT image pixel and fitted the global P-V curves to five sigmoid model equations to determine the LPMC, inflection point (IP) and upper point of maximal curvature (UPMC). Points of maximal curvature and IP were compared between the models by one-way analysis of variance (ANOVA). The percentages of lung pixels remaining closed (“unrecruited lung”) at LPMC, IP and UPMC were calculated from the number of lung pixels exhibiting regional opening pressures higher than LPMC, IP and UPMC and were also compared by one-way ANOVA. As results, we found a high variability of LPMC values among the models, a smaller variability of IP and UPMC values. We found a high percentage of unrecruited lung at LPMC, a small percentage of unrecruited lung at IP and no unrecruited lung at UPMC. Our results confirm the notion of ongoing lung recruitment at pressure levels above LPMC for all investigated model equations and highlight the importance of a regional assessment of lung recruitment in patients with ARDS.

Keywords: EIT, mechanical ventilation, ARDS, pressure-volume curve, respiratory mechanics, lung recruitment, sigmoid models.

1. Introduction

Repeated opening and closing of alveoli, also known as “tidal recruitment”, is one of the most important factors contributing to ventilator-induced lung injury in patients suffering from acute respiratory distress syndrome (ARDS). It can, in part, be prevented by adequate positive end-expiratory pressure (PEEP) (Dreyfuss and Saumon, 1998; Caironi *et al.*, 2010). Static or quasi-static pressure-volume (P-V) curves can be used to identify the PEEP levels at which tidal recruitment is reduced and to adjust the ventilator accordingly (Amato *et al.*, 1995; Ranieri *et al.*, 1999). According to the traditional interpretation, tidal recruitment occurs mainly below the lower point of maximum curvature (LPMC, often referred to as the “lower inflection point” in the medical literature) of the P-V curve. This assumption has been challenged by mathematical (Hickling, 1998), experimental (Pelosi *et al.*, 2001) and clinical (Crotti *et al.*, 2001; Albaiceta *et al.*, 2004) studies, emphasizing the regional differences in lung recruitment and derecruitment in patients with ARDS. According to this new interpretation first introduced by Hickling (1998), opening of alveoli continues during the linear part of the P-V curve and the curve’s inflection point (IP) and diminishes around the upper point of maximal curvature (UPMC) of the curve. Nevertheless, besides a reduction in tidal volume, setting of positive end-expiratory pressure (PEEP) 2 cmH₂O above the LPMC was one of the key components of the “lung-protective” ventilation strategy that improved lung function and survival of patients suffering from ARDS in several clinical studies (Amato *et al.*, 1995; Amato *et al.*, 1998; Villar *et al.*, 2006). These findings could, in part, be explained by the reduction in tidal recruitment that was promoted by applying the “lung-protective” strategy.

In clinical practice, the visual identification of the points of maximal curvature is associated with a high intra- and inter-observer variability (Harris *et al.*, 2000). To overcome this limitation, mathematical models describing the P-V curve have been proposed. The first and most commonly used model was described by Venegas *et al.* (1998). It consists of a sigmoid equation symmetric around the IP of the curve:

$$V(P) = a + \frac{b}{1 + e^{-\frac{P-c}{d}}} \quad (1)$$

This model was simplified by Pelosi *et al.* (2001), assuming the lower asymptote to be equal to 0, reducing the potential fitting error:

$$V(P) = \frac{b}{1 + e^{-\frac{P-c}{d}}} \quad (2)$$

To allow for a more smooth fitting, a 5th fitting parameter was introduced by Heller *et al.* (2002):

$$V(P) = a + \frac{b}{\left(1 + e^{-\frac{P-c}{d}}\right)^5} \quad (3)$$

An approach to allow the fitting of asymmetric data was proposed by Henzler *et al.* (2003):

$$V(P) = \frac{V_0 - V_0 e^{-kP}}{1 + e^{-\frac{P-c}{d}}} \quad (4)$$

A comparative study by Albaiceta and coworkers has shown that the above models, while all showing an excellent goodness of fit, yield conflicting results regarding LPMC and UPMC when fitted to P-V curve data from patients with ARDS (Albaiceta *et al.*, 2007). This could, in part, be explained by ongoing lung recruitment above LPMC, caused by the high variability of regional opening pressures across the lung. Lung recruitment above LPMC has been confirmed in small groups of ARDS patients using computed tomography (CT) imaging of a single lung slice and static inflation methods to construct the P-V curve (Crotti *et al.*, 2001; Albaiceta *et al.*, 2004) but, to our knowledge, never using the clinically preferable sustained-inflation technique.

Electrical impedance tomography (EIT) can be used for continuous determination of regional gas volume changes in the lungs (Frerichs *et al.*, 2016). This allows the assessment of regional opening and closing pressures in patients with ARDS during a sustained-inflation P-V manoeuvre (Pulletz *et al.*, 2012). Using this method, lung areas remaining unrecruited at a given airway pressure can be identified.

The aim of our present study was to better characterise the ongoing lung recruitment during a sustained-inflation P-V loop by quantifying the percentage of lung pixels remaining unrecruited at LPMC, IP and UPMC. We furthermore thought to quantify the differences between the different sigmoid models regarding the percentage of unrecruited lung at LPMC, IP and UPMC.

2. Methods

We retrospectively included patients from a database containing 44 cases previously enrolled in two clinical studies (Pulletz *et al.*, 2012; Becher *et al.*, 2014). For the present study, only data from patients who fulfilled the criteria for ARDS according to the Berlin definition (Ranieri *et al.*, 2012) were analysed.

The patients were ventilated with the Evita XL ventilator (Drägerwerk, Lübeck, Germany) and EIT data were obtained with the GOE-MF-II device (CareFusion, Yorba Linda, USA) at a scan rate of 25 images per second. For acquisition of EIT data, 16 self-adhesive electrodes (Blue-Sensor L-00-S, Ambu, Ballerup, Denmark) were placed around the patient's chest circumference in one transverse plane at the level of the 4th to 5th intercostal space, measured in the parasternal line. Ventilation data and EIT data were recorded during a standardized quasi-static P-V manoeuvre. It was performed with the sustained-inflation method using a continuous gas flow of 4 l/min, starting at the airway pressure of 0 cmH₂O up to the maximum pressure of 35 cmH₂O or a maximum volume of 2 l. Airway pressure, gas flow and tidal volume were measured by the ventilator at a scan rate of 125 Hz and stored on a laptop computer.

2.1. Regional opening pressures

For assessment of regional opening pressures, cross-sectional images were calculated from the acquired EIT data using a time-difference reconstruction algorithm based on GREIT (Adler *et al.*, 2009). A functional region of interest (ROI) was identified using a threshold criterion of 25% of the maximum conductivity change. For each pixel in the ROI, its conductivity time course was fitted to a fourth-order polynomial. Subsequently, the time at which the fitted conductivity curve crossed 10% of its maximum conductivity change was identified and the corresponding airway pressure was determined as regional opening pressure (ROP). This procedure is explained in detail in (Pulletz *et al.*, 2012).

2.2. Sigmoid model fittings

To identify the different sigmoid models, the pressure and volume data measured by the ventilator were fitted to equations 1-4 using a nonlinear least squares regression. We furthermore modified equation 3, assuming the lower asymptote to be equal to zero:

$$V(P) = \frac{b}{\left(1 + e^{-\frac{P-c}{d}}\right)^s} \quad (5)$$

The fittings were performed with a Nelder-Mead Simplex Algorithm using Matlab 2014a (The MathWorks Inc., Natick, USA).

As described by Albaiceta *et al.* (2007), LPMC and UPMC for equations 1 and 2 were determined as

$$LPMC = c - 1.317d \quad (6)$$

$$UPMC = c + 1.317d. \quad (7)$$

For equations 3 and 5, LPMC and UPMC were calculated according to

$$LPMC = c - d \ln \frac{(3s+1) - \sqrt{5*s^2+6s+1}}{2s^2} \quad (8)$$

$$UPMC = c - d \ln \frac{(3s+1) + \sqrt{5*s^2+6s+1}}{2s^2}. \quad (9)$$

For equation 4, the maximum and minimum of the second derivative, corresponding to LPMC and UPMC, were calculated numerically after computing a second-order approximation of the second derivative of the fitted model.

The IP of the curve is equal to c for equations 1, 2, 3 and 5. For equation 4, it was calculated numerically as the maximum of the first derivative after computing a second-order approximation of the first derivative of the fitted model.

Figure 1 shows one representative P-V curve fitted to the five models and the corresponding regional opening pressure map.

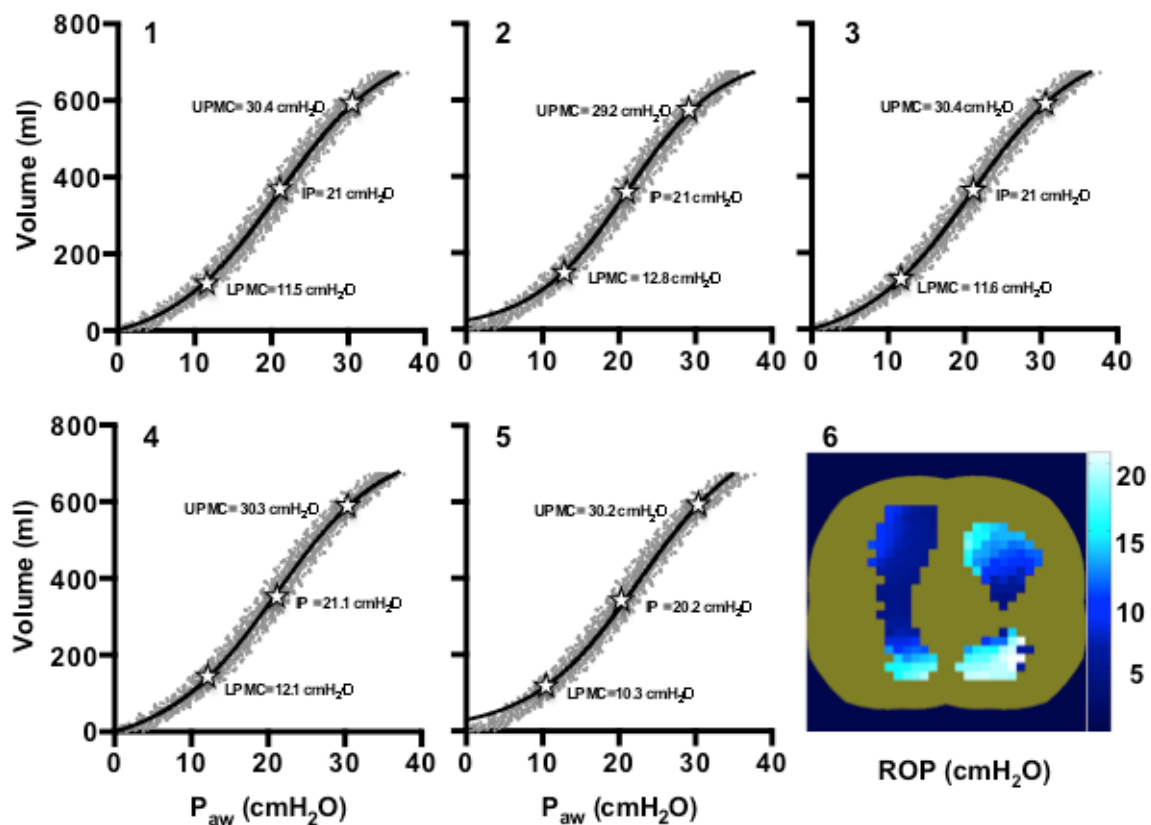


Figure 1 Panels 1 - 5: Pressure-volume curve from one representative patient with ARDS, fitted to models 1 - 5, respectively. Raw data are shown as grey dots, the black lines represent the results of the model fits. The asterisks denote the lower point of maximum curvature (LPMC), the inflection point

(IP) and the upper point of maximum curvature (UPMC). Panel 6: Regional opening pressures obtained from the same patient.

2.3 Percentage of unrecruited pixels at points of maximum curvature and inflection point

Any image pixel exhibiting a higher ROP value than the model-derived global LPMC, IP or UPMC was defined as „unrecruited“ at the corresponding airway pressure. The percentage of unrecruited lung at IP and the points of maximal curvature was calculated for each model from the number of image pixels with ROP values higher than LPMC, IP and UPMC, divided by the whole number of image pixels within the ROI. Additionally, we calculated the percentage of unrecruited lung at the clinically recommended pressure level corresponding to LPMC + 2 cmH₂O in the same way. This analysis was conducted in Microsoft Excel 2011 (Microsoft, Seattle, USA).

2.4 Statistical analysis

Statistical analyses were performed using GraphPad Prism 6.0 (GraphPad Software, LaJolla, USA). The LPMC, IP and UPMC values and the percentages of unrecruited lung for the different models were compared using a one-way analysis of variance for repeated measures and Bonferroni's multiple comparisons test. The agreement between models was tested by dividing the sum-of-squares between individual subjects by the total sum-of-squares, reporting the result as r^2 . To assess whether the agreement between models was statistically significant, the effectiveness of the matching between the different models was tested with an F test, reporting the resulting p value. P values < 0.05 were considered statistically significant. Numerical values are presented as mean \pm standard deviation unless specified otherwise.

3. Results

In total, 30 patients (23 male, 7 female, age: 59 ± 16 years, height 174 ± 8 cm, weight 81 ± 15 kg) fulfilled ARDS criteria and were included in the subsequent analyses. The investigated patients were ventilated with an inspired fraction of oxygen (FiO₂) of 0.61 ± 0.17 , a tidal volume of 8.0 ± 1.7 ml / kg predicted body weight and a PEEP level of 12 ± 4 cmH₂O. The average PaO₂/FiO₂ – ratio was 173 ± 50 mmHg and the global respiratory system compliance 53 ± 19 ml / cmH₂O.

The average root mean square (RMS) values of the residues in the different model fits are shown in table 1.

Venegas et al. (1)	Pelosi et al. (2)	Heller et al. (3)	Henzler et al. (4)	modified (5)
33.8ml	49.0ml	38.2ml	35.4ml	38.3ml

Table 1 Root mean square values for the residues in the different model fits.

3.1 Points of maximal curvature and inflection point with different models

There was a significant matching but only a moderate agreement between LPMC values obtained with the different models ($r^2 = 0.62$, $p < 0.0001$). With a mean LPMC value of 11.6 ± 2.4 cmH₂O, model 2 showed significantly higher results in comparison to all other models (model 1: 6.8 ± 5.3 cmH₂O; model 3: 7.2 ± 2.9 cmH₂O; model 4: 8.2 ± 3.3 cmH₂O; model 5: 7.7 ± 2.5 cmH₂O).

Regarding IP, we found a significant matching and an excellent agreement between the values obtained with the five models ($r^2 = 0.94$, $p < 0.0001$). Multiple comparisons revealed a small but statistically significant differences in IP values between models 1 and 4 (model 1: 19.1 ± 4.3 cmH₂O; model 4: 18.3 ± 4.3 cmH₂O) and between models 2 and 5 (model 2: 19.2 ± 3.0 cmH₂O; model 5: 18.5 ± 3.6 cmH₂O). IP identified with Model 3 (18.5 ± 3.8 cmH₂O) did not differ significantly from any other model.

For UPMC, there was a significant matching and a relatively good agreement between the different model values ($r^2 = 0.81$; $p < 0.0001$). UPMC was identified at 31.6 ± 5.8 cmH₂O for model 1, 26.7 ± 3.9 cmH₂O for model 2, 29.8 ± 5.8 cmH₂O for model 3, 27.3 ± 6.9 cmH₂O for model 4 and at 29.2 ± 5.4 cmH₂O for model 5. Using multiple comparisons, statistically significant differences were identified between models 1 and 2, models 1 and 4, models 1 and 5, models 2 and 3, models 2 and 5, models 3 and 4 and between models 4 and 5.

The results for LPMC, IP and UPMC obtained with the different models are presented in figure 2.

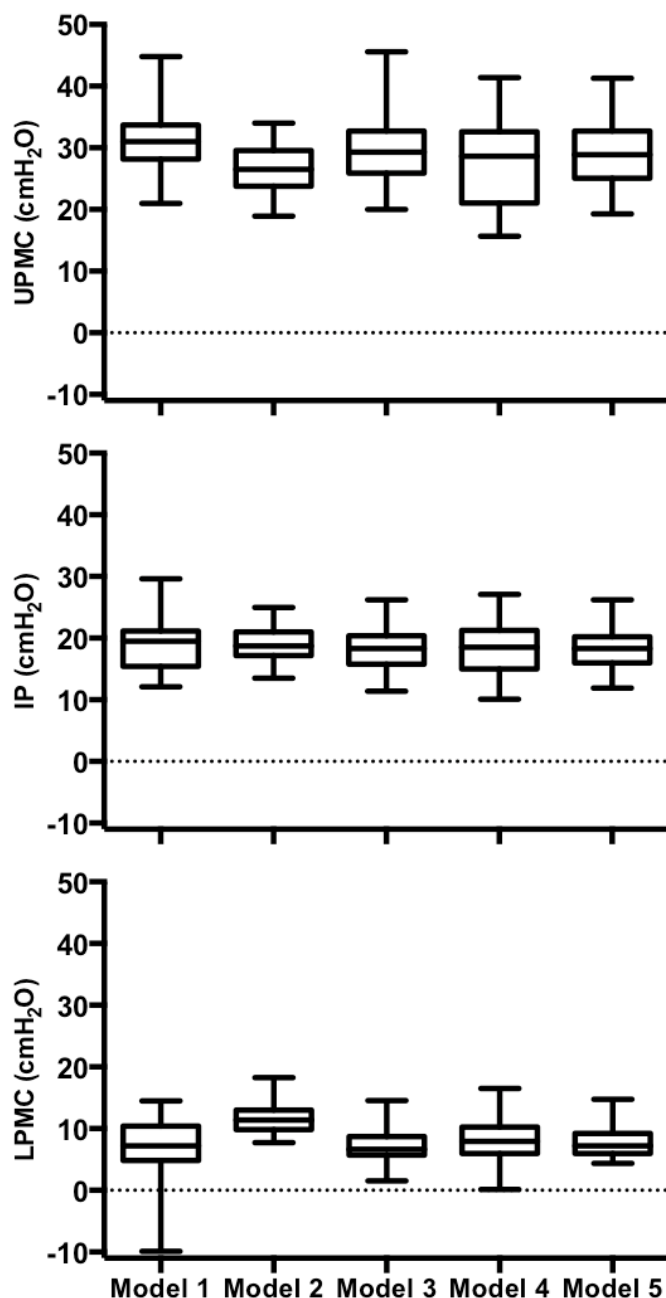


Figure 2 Lower points of maximum curvature (LPMC), inflection points (IP) and upper points of maximum curvature (UPMC), identified with the different sigmoid model equations. Box and whisker plots show the maximum, 75th percentile, median, 25th percentile and minimum values.

3.2 Percentage of unrecruited lung at points of maximal curvature and inflection point.

We identified unrecruited lung pixels at all LPMC values. The percentage of unrecruited lung at LPMC found with model 2 (14 ± 12 %) was significantly lower than the percentages found with all

other models (model 1: 57 ± 33 %; model 3: 59 ± 26 %; model 4: 50 ± 26 ; model 5: 53 ± 22 %). No significant differences in percentage of unrecruited lung at LPMC were observed between models 1, 3, 4 and 5. Similar results were obtained at an airway pressure corresponding to LPMC + 2 cmH₂O (model 1: 29 ± 25 %; model 2: 4 ± 4 %; model 3: 28 ± 17 %; model 4: 20 ± 17 %; model 5: 22 ± 14 %). At the pressure corresponding to IP, we found only very small percentages of unrecruited lung, with average values of 0.5 ± 1.4 %, 0.2 ± 0.5 %, 0.4 ± 1.0 %, 0.6 ± 1.4 % and 0.4 ± 1.0 % for models 1-5, respectively and no significant differences in percentage of unrecruited pixels between the five models. No unrecruited lung was identified at the airway pressure corresponding to UPMC. The percentages of unrecruited pixels at LPMC and IP are presented graphically in figure 3. In addition, the percentage of unrecruited pixels at LPMC is plotted against the pressure at LPMC for all patients in figure 4.

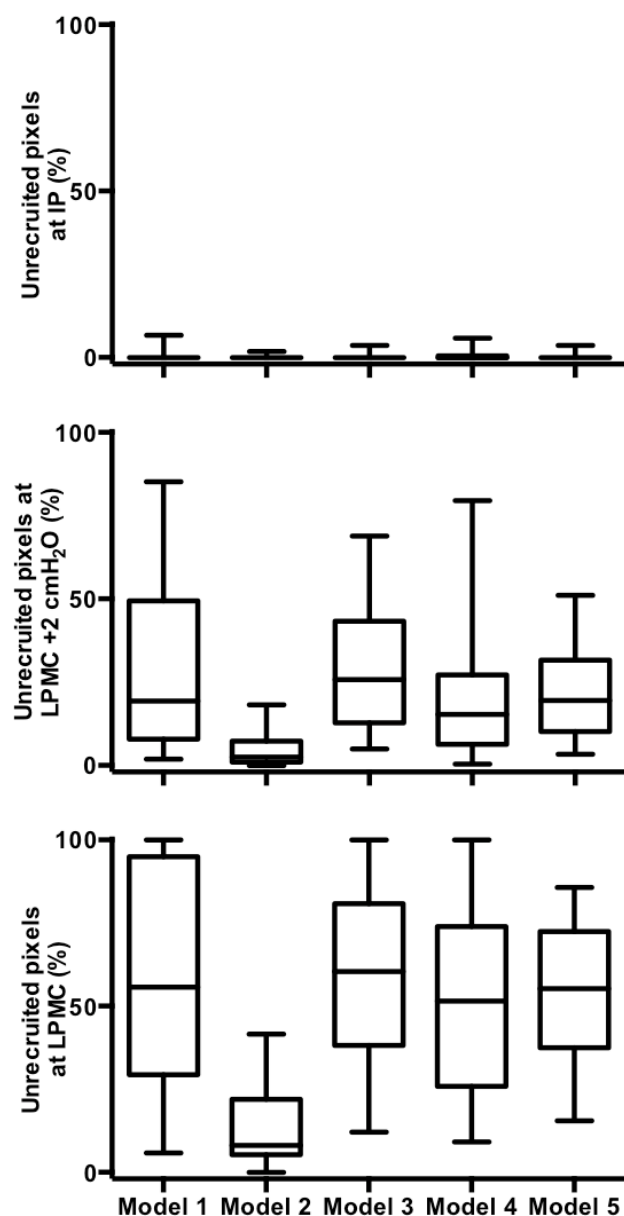


Figure 3 Percentage of unrecruited pixels at the airway pressure corresponding to the lower point of maximum curvature (LPMC), 2 cmH₂O above LPMC (LPMC + 2 cmH₂O) and the inflection point (IP), identified by the different sigmoid model equations. Box and whisker plots show the maximum, 75th percentile, median, 25th percentile and minimum values.

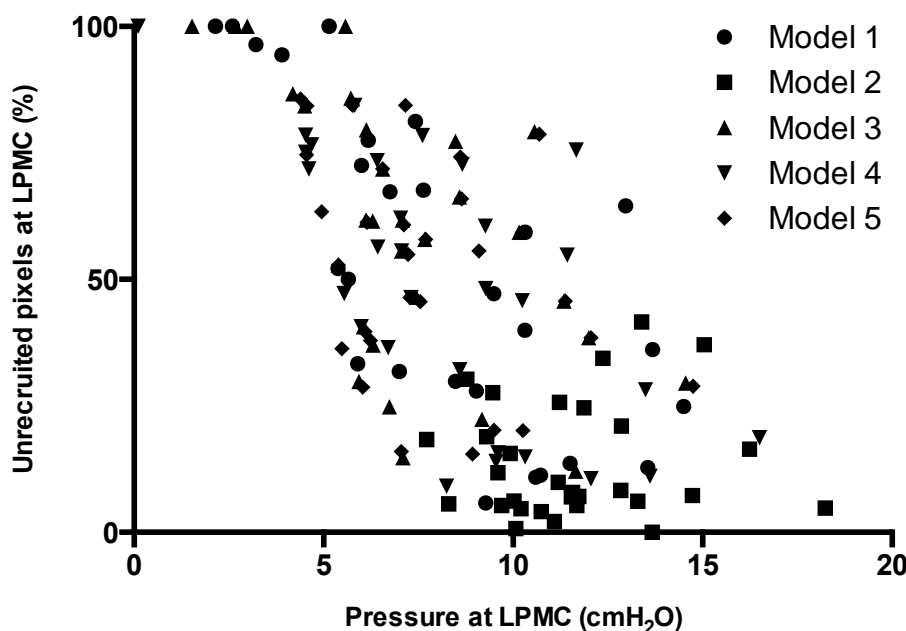


Figure 4 Percentage of unrecruited pixels at the airway pressure corresponding to the lower point of maximum curvature (LPMC), plotted against the corresponding airway pressure for all investigated models. 3 data points with negative values for pressure at LPMC were derived using Model 1 and are not shown in this figure.

4. Discussion

In the present study, we assessed the relationship between five sigmoid models for the global description of sustained-inflation P-V curves with the EIT-derived regional opening pressures in 30 patients suffering from ARDS. For all models, we detected high percentages of lung pixels remaining closed at airway pressures corresponding to LPMC, small percentages of lung pixels remaining closed at airway pressures corresponding to IP and no lung pixels remaining closed at airway pressures corresponding to UPMC. At the clinically recommended pressure level of LPMC + 2 cmH₂O, relevant percentages of unrecruited lung pixels were found for all models with the exception of model 2, which lead to significantly higher LPMC values in comparison with all other models. These findings are in accordance with the ongoing recruitment above LPMC proposed by Hickling (1998). Previously published studies providing evidence of recruitment above LPMC used no imaging method (Jonson *et al.*, 1999; Richard *et al.*, 2001) or investigated a static P-V manoeuvre with continuous positive airway pressure or the “super-syringe” technique (Pelosi *et al.*, 2001; Crotti *et al.*, 2001; Albaiceta *et al.*, 2004) in relatively small groups of animals and patients. Our results confirm the findings of the aforementioned studies in a larger group of patients during a sustained-inflation P-V manoeuvre.

Since lung-volume history can greatly influence the shape of an ascending P-V curve, it is important to point out that no high-pressure recruitment maneuvers or PEEP titrations were performed prior to the measurement. Before the P-V maneuvers, all patients were ventilated using clinically selected settings for PEEP and tidal volume as stated in the results section.

Comparing the different sigmoid models, we found a high degree of variability in LPMC values, confirming the previous results found in a different patient population (Albaiceta *et al.*, 2007). Model 2 showed significantly higher LPMC values than the other models. This is due to the fact that model 2 is a modification of model 1, with the simplification of the lower asymptote being assumed to be equal to zero. The higher LPMC values that were obtained with model 2 explain the observed lower percentages of unrecruited image pixels at the pressure levels corresponding to LPMC and LPMC + 2 cmH₂O according to model 2. As can be seen in figure 1, the model fit appeared to be less accurate in the lower pressure range for models 2 and 5, a phenomenon that is most likely explained by the lower asymptote being forced to zero. This could also explain the lower overall goodness of fit obtained for model 2. Nonetheless, we believe that the simplification of assuming the lower asymptote to be equal to zero may be justified from a physiological point of view and could improve the results by reducing the number of parameters in the fit. For instance, in contrast to model 1, no negative values of LPMC

were obtained with model 2 and the percentage of unrecruited image pixels at the clinically recommended PEEP level of LPMC + 2 cmH₂O was smaller than with the more complex models. Therefore, the results for LPMC obtained with model 2 seem to be more physiologically plausible than the ones obtained with model 1. Still, the relatively low overall goodness of fit obtained for this model warrants caution when using it for PEEP adjustment in clinical practice.

Regarding IP, we found a relatively low variability between the models. The small but statistically significant differences in IP between models 1 and 4 and between models 2 and 5 lead to no significant difference in percentage of unrecruited image pixels at IP and can be considered as clinically insignificant, being smaller than 1 cmH₂O on average.

For UPMC, we found a higher variability between the models than for IP but a lower variability than for LPMC. Model 2, which yielded the highest values for LPMC, yielded the lowest values for UPMC in our analysis.

A possible interpretation of these results is that the high degree of ongoing recruitment at pressure levels to LPMC lead to the high variability in LPMC values identified with the different models. According to our results, the majority of recruitment was completed at pressure levels above IP. This could, in part, explain the lower variability of IP and UPMC values identified with the different models. One could therefore conclude that, if no regional assessment of lung recruitment is available, adjusting PEEP according to the true inflection point (IP) of the P-V curve could be a better strategy than using the LPMC for PEEP adjustment. This approach warrants further investigation before being introduced into clinical practice.

EIT-derived maps of P-V curve shapes are a newly proposed approach for detection of tidal recruitment and overdistension that could possibly be used to guide mechanical ventilation in the future (Beda *et al.*, 2017). A recently proposed recruitment function could also be applied to identify the recruited volume at a given airway pressure (Uzawa *et al.*, 2015) but requires further validation in human patient data.

Our study has some important limitations. First, when interpreting our data, one must be aware of the relatively poor spatial resolution of EIT images. It is likely that in some cases, open and closed lung areas may have been included within one EIT image pixel. In this case, the inflation of already open lung areas within the affected image pixel would overlay the areas remaining closed at the same airway pressure. This would cause an underestimation of the regional opening pressures with our EIT-based method and therefore an overestimation of recruited lung tissue at a given level of airway pressure. The limited pressure and volume range that was used for the P-V curve (maximum airway pressure 35 cmH₂O, maximum inspiratory volume 2 l) can be considered another limitation of our results. In some cases, recruitment could continue at an airway pressure above 35 cmH₂O. This would also lead to an underestimation of the “true” regional opening pressure with our method. The limited pressure and volume range was chosen for safety reasons to avoid barotrauma and volutrauma caused by the P-V manoeuvre.

Also, we did not use a reference method like CT to validate the results obtained for the regional lung opening and the ROP method has never been validated against CT. This is due to the fact that we consider exposing a patient to the high dose of radiation associated with repeated CT scan for research purposes as unethical. Also, the low temporal resolution of CT could impede the assessment of a sustained-inflation P-V loop. Nevertheless, there are numerous experimental and clinical studies comparing EIT and CT scans, showing a good agreement between the methods (Costa *et al.*, 2009; Wrigge *et al.*, 2008; Muders *et al.*, 2012; Yoshida *et al.*, 2013; Elke *et al.*, 2013).

Furthermore, the investigated models are nonlinear with respect to the parameters. This leads to cross-terms among parameters in the cost function to be minimized which may give rise to cost functions with (possibly many) local minima. Minimization algorithms may therefore stop at different points depending on the starting points (“initial guesses”). It has to be noted that the evaluation for this study was done using local optimal solutions. Nevertheless, we performed tests using various different starting points which usually converged to the same local minima for the models employed here. We therefore believe that the overall conclusion remains valid despite these short comings.

It must also be noted that the pressure data we used to identify our models were acquired at the airway opening. Adding esophageal pressure data to calculate transpulmonary pressure and using transpulmonary P-V curves for model identification might have improved the results of the model fittings with respect to the patient’s actual lung mechanics.

Due to the diffuse nature of electrical current propagation within the human body, the exact volume of lung tissue that is contained within one image pixel cannot be quantified exactly. It should therefore be noted that our analysis was „quantitative“ with respect to the percentage of lung pixels remaining unrecruited at a certain fiducial point, but only semi-quantitative concerning the corresponding lung volume.

Last, our study was a retrospective data analysis. Since all the P-V curves were obtained with the same ventilator settings and the acquisition and analysis of EIT and ventilator data was identical for all patients, making the results comparable.

In conclusion, we presented a semi-quantitative assessment of ongoing lung recruitment during a sustained-inflation P-V manoeuvre. We found a considerable variability of LPMC values identified with the different sigmoid model equations which was associated with a variable percentage of unrecruited lung pixels at the corresponding values of airway pressure. The variability of IP and UPMC values derived from the different model equations was relatively small. These findings could, in part, be explained by the higher amount of ongoing lung recruitment at airway pressures corresponding to LPMC. Our results underline the limitations of a global analysis of the P-V curve. We therefore conclude that a regional assessment of lung recruitment in patients with ARDS should be preferred over a global analysis of the P-V curve.

Abbreviations

ANOVA	Analysis of Variance
ARDS	Acute Respiratory Distress Syndrome
CT	Computed Tomography
EIT	Electrical Impedance Tomography
FiO ₂	Inspired Fraction of Oxygen
IP	Inflection Point
LPMC	Lower Point of Maximum Curvature
PaO ₂	Arterial Partial Pressure of Oxygen
PEEP	Positive End-Expiratory Pressure
P-V	Pressure-Volume
ROI	Region of Interest
ROP	Regional Opening Pressure
UPMC	Upper Point of Maximal Curvature

References

- Adler A, Arnold J H, Bayford R, Borsic A, Brown B, Dixon P, Faes T J, Frerichs I, Gagnon H, Garber Y, Grychtol B, Hahn G, Lionheart W R, Malik A, Patterson R P, Stocks J, Tizzard A, Weiler N and Wolf G K 2009 GREIT: a unified approach to 2D linear EIT reconstruction of lung images *Physiol Meas* **30** S35-55
- Albaiceta G M, Garcia E and Taboada F 2007 Comparative study of four sigmoid models of pressure-volume curve in acute lung injury *Biomed Eng Online* **6** 7
- Albaiceta G M, Taboada F, Parra D, Luyando L H, Calvo J, Menendez R and Otero J 2004 Tomographic study of the inflection points of the pressure-volume curve in acute lung injury *Am J Respir Crit Care Med* **170** 1066-72
- Amato M B, Barbas C S, Medeiros D M, Magaldi R B, Schettino G P, Lorenzi-Filho G, Kairalla R A, Deheinzelin D, Munoz C, Oliveira R, Takagaki T Y and Carvalho C R 1998 Effect of a protective-ventilation strategy on mortality in the acute respiratory distress syndrome *N Engl J Med* **338** 347-54
- Amato M B, Barbas C S, Medeiros D M, Schettino Gde P, Lorenzi Filho G, Kairalla R A, Deheinzelin D, Morais C, Fernandes Ede O, Takagaki T Y and et al. 1995 Beneficial effects of the "open lung approach" with low distending pressures in acute respiratory

- distress syndrome. A prospective randomized study on mechanical ventilation *Am J Respir Crit Care Med* **152** 1835-46
- Becher T H, Bui S, Zick G, Blaser D, Schadler D, Weiler N and Frerichs I 2014 Assessment of respiratory system compliance with electrical impedance tomography using a positive end-expiratory pressure wave maneuver during pressure support ventilation: a pilot clinical study *Crit Care* **18** 679
- Beda A, Carvalho A R, Carvalho N C, Hammermuller S, Amato M B, Muders T, Gittel C, Noreikat K, Wrigge H and Reske A W 2017 Mapping Regional Differences of Local Pressure-Volume Curves With Electrical Impedance Tomography *Crit Care Med* **45** 679-86
- Caironi P, Cressoni M, Chiumello D, Ranieri M, Quintel M, Russo S G, Cornejo R, Bugedo G, Carlesso E, Russo R, Caspani L and Gattinoni L 2010 Lung opening and closing during ventilation of acute respiratory distress syndrome *Am J Respir Crit Care Med* **181** 578-86
- Costa E L, Borges J B, Melo A, Suarez-Sipmann F, Toufen C, Jr., Bohm S H and Amato M B 2009 Bedside estimation of recruitable alveolar collapse and hyperdistension by electrical impedance tomography *Intensive Care Med* **35** 1132-7
- Crotti S, Mascheroni D, Caironi P, Pelosi P, Ronzoni G, Mondino M, Marini J J and Gattinoni L 2001 Recruitment and derecruitment during acute respiratory failure: a clinical study *Am J Respir Crit Care Med* **164** 131-40
- Dreyfuss D and Saumon G 1998 Ventilator-induced lung injury: lessons from experimental studies *Am J Respir Crit Care Med* **157** 294-323
- Elke G, Fuld M K, Halaweish A F, Grychtol B, Weiler N, Hoffman E A and Frerichs I 2013 Quantification of ventilation distribution in regional lung injury by electrical impedance tomography and xenon computed tomography *Physiol Meas* **34** 1303-18
- Frerichs I, Amato M B, van Kaam A H, Tingay D G, Zhao Z, Grychtol B, Bodenstern M, Gagnon H, Bohm S H, Teschner E, Stenqvist O, Mauri T, Torsani V, Camporota L, Schibler A, Wolf G K, Gommers D, Leonhardt S and Adler A 2016 Chest electrical impedance tomography examination, data analysis, terminology, clinical use and recommendations: consensus statement of the TRanslational EIT developmeNt stuDY group *Thorax* **0**:1-11
- Harris R S, Hess D R and Venegas J G 2000 An objective analysis of the pressure-volume curve in the acute respiratory distress syndrome *Am J Respir Crit Care Med* **161** 432-9
- Heller H, Brandt S and Schuster K D 2002 Development of an algorithm for improving the description of the pulmonary pressure-volume curve *J Appl Physiol (1985)* **92** 1770; author reply -1
- Henzler D, Orfao S, Rossaint R and Kuhlen R 2003 Modification of a sigmoidal equation for the pulmonary pressure-volume curve for asymmetric data *J Appl Physiol (1985)* **95** 2183-4; author reply 4
- Hickling K G 1998 The pressure-volume curve is greatly modified by recruitment. A mathematical model of ARDS lungs *Am J Respir Crit Care Med* **158** 194-202
- Jonson B, Richard J C, Straus C, Mancebo J, Lemaire F and Brochard L 1999 Pressure-volume curves and compliance in acute lung injury: evidence of recruitment above the lower inflection point *Am J Respir Crit Care Med* **159** 1172-8
- Muders T, Luepschen H, Zinserling J, Greschus S, Fimmers R, Guenther U, Buchwald M, Grigutsch D, Leonhardt S, Putensen C and Wrigge H 2012 Tidal recruitment assessed by electrical impedance tomography and computed tomography in a porcine model of lung injury* *Crit Care Med* **40** 903-11
- Pelosi P, Goldner M, McKibben A, Adams A, Eccher G, Caironi P, Losappio S, Gattinoni L and Marini J J 2001 Recruitment and derecruitment during acute respiratory failure: an experimental study *Am J Respir Crit Care Med* **164** 122-30

- Pulletz S, Adler A, Kott M, Elke G, Gawelczyk B, Schadler D, Zick G, Weiler N and Frerichs I 2012 Regional lung opening and closing pressures in patients with acute lung injury *J Crit Care* **27** 323 e11-8
- Ranieri V M, Rubenfeld G D, Thompson B T, Ferguson N D, Caldwell E, Fan E, Camporota L and Slutsky A S 2012 Acute respiratory distress syndrome: the Berlin Definition *Jama* **307** 2526-33
- Ranieri V M, Suter P M, Tortorella C, De Tullio R, Dayer J M, Brienza A, Bruno F and Slutsky A S 1999 Effect of mechanical ventilation on inflammatory mediators in patients with acute respiratory distress syndrome: a randomized controlled trial *Jama* **282** 54-61
- Richard J C, Maggiore S M, Jonson B, Mancebo J, Lemaire F and Brochard L 2001 Influence of tidal volume on alveolar recruitment. Respective role of PEEP and a recruitment maneuver *Am J Respir Crit Care Med* **163** 1609-13
- Uzawa Y, Otsuji M, Nakazawa K, Fan W and Yamada Y 2015 Derivation of recruitment function from the pressure-volume curve in an acute lung injury model *Respir Physiol Neurobiol* **205** 16-20
- Venegas J G, Harris R S and Simon B A 1998 A comprehensive equation for the pulmonary pressure-volume curve *J Appl Physiol* **84** 389-95
- Villar J, Kacmarek R M, Perez-Mendez L and Aguirre-Jaime A 2006 A high positive end-expiratory pressure, low tidal volume ventilatory strategy improves outcome in persistent acute respiratory distress syndrome: a randomized, controlled trial *Crit Care Med* **34** 1311-8
- Wrigge H, Zinserling J, Muders T, Varelmann D, Gunther U, von der Groeben C, Magnusson A, Hedenstierna G and Putensen C 2008 Electrical impedance tomography compared with thoracic computed tomography during a slow inflation maneuver in experimental models of lung injury *Crit Care Med* **36** 903-9
- Yoshida T, Torsani V, Gomes S, De Santis R R, Beraldo M A, Costa E L, Tucci M R, Zin W A, Kavanagh B P and Amato M B 2013 Spontaneous effort causes occult pendelluft during mechanical ventilation *Am J Respir Crit Care Med* **188** 1420-7